Evaluating Barrier Properties Of Organic Coatings by Water Permeation And Electrochemical Methods

P.C. Inone and C.M. Garcia—Instituto de Tecnologia para o Desenvolvimento*
A. Rúvolo-Filho—Universidade Federal de São Carlos*

Water permeation, water absorption, d.c. resistance, and electrochemical impedance spectroscopy (EIS) measurements were performed on films of epoxy-polyamide used as binder in paint formulations. Barrier properties were found to be highly dependent upon the thickness of films. In thick films, water permeation measurements revealed the presence of pathways attributed to frozen holes, through which the flow is not governed by diffusion. In thin films, the presence of pinholes was detected by d.c. resistance and EIS measurements.

INTRODUCTION

Organic coatings protect metals against corrosion by various mechanisms,[1] which can be summarized as follows: (a) suppression of the anodic and/or cathodic reaction, (b) the introduction of a high electrical resistance into the circuit of the corrosion cell, and (c) a barrier to aggressive species (oxygen, water, and ions).

Measurement of ionic resistance by the polarization method has been used successfully for many years as a method to characterize paints and varnishes.[2-8] Briefly, good performance is recognized if a high d.c. resistance is observed when the coating is exposed to an electrolyte solution. In these studies, it was stated that coatings frequently contain areas of low ionic resistance named D-type areas and areas of high ionic resistance named I-type areas. The predominance of either kind of these areas determines the total ionic resistance of a coating.

Today, electrochemical impedance spectroscopy (EIS) is preferred to evaluate the performance of organic coatings because it allows for a more complete characterization. For instance, the uptake of ions into the coatings has been related to the increase in d.c. resistance of the coatings,[1,9-11] while the uptake of water has been related to the increasing capacitance of the coatings.[12,13] Also, EIS has been used to estimate the degree of delamination.[14,15]

According to Szauer,[16] coatings can be classified into four groups. The first group is made up of those coatings that act like dielectrics and barrier materials. Failure of these materials to protect the substrate arises from the penetration of conductive solutions into the coating by diffusion. The second group of coatings includes those possessing conductive pathways, which usually allow immediate contact between metal and electrolyte solution. Commercial paints usually produce coatings with pores and fissures that originated during the evaporation of solvents and atmospheric exposure. All of these discontinuities have to be considered as potential conductive paths when in contact with an electrolyte solution. The third group includes those very porous, fissured, or well-conducting coatings, including those of advanced degradation, where the capacitive effect of the coating may be disregarded. The fourth group is constituted by some hydrocarbon-based oils and protective coatings, whose hydrophobic nature, as well as lack of pores and fissures, gives them the char-

*LACTEC, Área de Materiais – AMAT, Caixa Postal 19067, CEP 81531–990, Curitiba, Paraná, Brazil.
Departamento de Química, Grupo de Processamento e Propriedades em Polímeros, Caixa Postal 676, CEP 13560-905, São Carlos, São Paulo, Brazil.

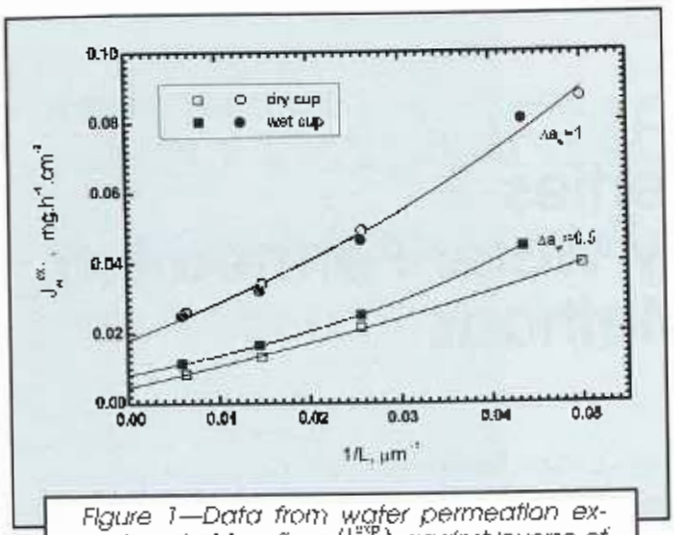

Figure 1—Data from water permeation experiments. Mass flow (U_w^{exp}) against inverse of the thickness of films.

acteristic of dielectric and barrier materials, even if applied in thin layers. When these coatings are exposed to an electrolyte solution they perform as a barrier for a relatively long time, but when this feature is lost they become penetrated quite rapidly.

A comprehensive review of degradation processes of paint films and the resultant corrosion processes at the interface film-substrate is given by Nguyen et al.[17] From results found in the literature, they proposed a unified model, where the degradation of defect-free organic coatings is initiated by conductive pathway formation and provoked by water attack (e.g., hydrolysis and dissolution) at hydrophilic regions that contain low-molecular weight/low-crosslinked materials. Such regions take up a large amount of water, leading to the formation and opening of pathways through the coating. Following this step, degradation advances by transport of water, oxygen, and ions through the formed pathways, from the environment to the metal surface. These authors also suggested that superposition of several thin layers of films should give rise to a highly impermeable coating due to the covering of pathways of a given layer by the subsequent layer, i.e., there would be an increase in the tortuosity of transport pathways in the coatings.

In view of that discussion, the purpose of this work is to further investigate the present knowledge about the performance of organic coatings, from a combined study of water transport, d.c. resistance measurements, and EIS measurements carried out in epoxy-polyamide varnish films. The effect of thickness on the behavior of these materials is investigated from the point of view of a multilayered model, where a single film of high thickness would be equivalent to one constituted by the superposition of several thin films.

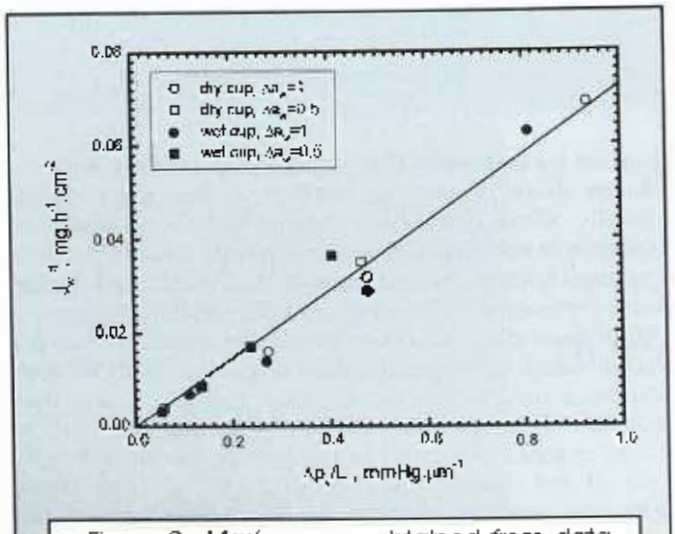

Figure 2—Master curve obtained from data of Figure 1.

EXPERIMENTAL

Materials

The epoxy resin studied was the diglycidyl ether of bisphenol A, as we verified by the FTIR spectra of the material received from Tintas Renner S.A. Cure was carried out by the addition of an equivalent weight of a polyamide cure agent (Versamid 115). The system was diluted to 70% w/w in a mixture 1/1 of xylene/isophurone in order to obtain a varnish with a viscosity adequate enough to be applied by an extension bar.

Sample Preparation

Free films used in studies of transport properties and d.c. resistance measurements were prepared by casting the epoxy-polyamide varnish with a variable extension bar onto glass plates. Attached films used in d.c. resistance and EIS measurements were prepared by casting the varnish onto nongalvanized carbon steel plates, which were previously sandblasted. After casting, the films were cured at room temperature in a closed chamber for four days and then further cured for 24 hr in an oven at 80°C. An almost complete crosslinking of the material was obtained with this rigorous treatment, as we verified from solvent extraction measurements. Free films were detached from the glass plates after immersion in distilled water for about three days, dried between two sheets of absorbent paper, and then kept on a desiccator containing silica gel.

Water Permeation

Water permeation was performed with the weighed-cell technique, in which the film is used to cap an open aluminum cup, thus functioning as a partition element between the interior and exterior of the cup. In "wet cup experiments," pure water or $CaCl_2$ solution with a known activity is put into the cup and the resulting set (cup, water/solution, and film) is placed upside down in a chamber under dry atmosphere, which is achieved

by placing a pot containing a strong desiccant (P_2O_5) inside the chamber. Under these conditions, a water activity difference (or equivalently, a water vapor pressure difference) is established between the inside and outside of the cup, so that water is forced to permeate the film, from inside to outside. By periodically weighing the cup, the loss of mass is obtained over time, which allows for the determination of water flow through the film. In "dry cup experiments," desiccant P_2O_5 is put into the cup, which, after being capped with the film, is placed upright in a chamber whose humidity is controlled by placing a pot containing pure water or $CaCl_2$ solution with a known activity. Under these conditions, water is forced to permeate the film from outside to inside. In this case, water flow through the film is measured by following the mass gain over time.

Water Sorption

Water sorption was measured by soaking discs of films with 37 mm diameters in pure water or NaCl solutions with variable activities over a period of a week. Although a day is sufficient for the films to take up a maximum quantity of water as was verified from previous tests, we kept them immersed for a week in order to wash out impurities like entrapped solvents inside the films. After that, the films were dried between two filter papers, weighed, and then dried in an oven at 80°C for 24 hr. By weighing the films again, the water uptake could be calculated as g/100 g of dry film. Further drying for another 24 hr did not produce any change in the weight of the films.

D.C. Resistance

D.C. resistance was measured by the polarization method. Free films were "sandwiched" between two halves of a cell, both of which were filled with NaCl solution. A platinum wire introduced into each compartment of the cell was used to make electrical contact with the solution. A potential of 0.6 volts was applied to the electrodes and the resistance was obtained by measuring the current.

Electrochemical Impedance Spectroscopy

EIS measurement was performed on the attached films. PVC cylinders with 21 mm internal diameters and 30 mm lengths were bound with adhesive onto the cured films. This set constituted the measurement cell, with the steel plate acting as a working electrode. A platinum strip was used as a counter electrode and a calomel electrode was used as a reference electrode. The cells were filled with an NaCl solution from 3M and then EIS measurements were performed over time. A potentiostat/galvanostat from EG&G Instruments and a frequency response analyzer from Solartron Instruments were used. Before each EIS measurement, the rest potential was measured and the value found was used as an imposed signal amplitude. The signal frequency range chosen was 1 MHz to 100 mHz, but in many cases the measurement was interrupted before the end because the response signal was prone to great error at low frequency.

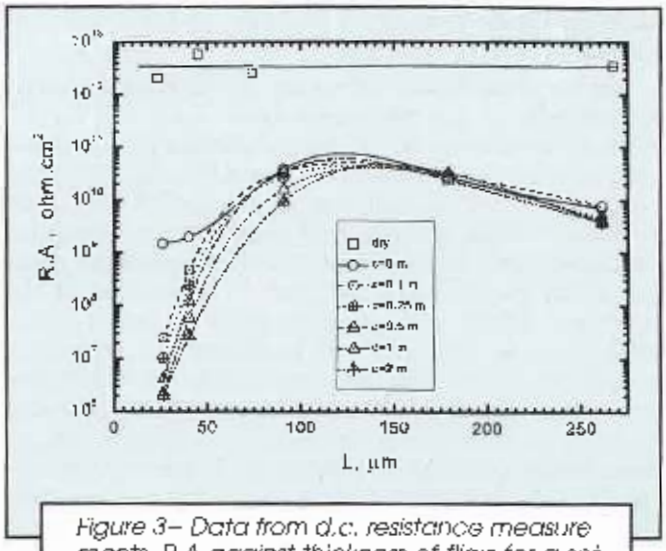

Figure 3– Data from d.c. resistance measurements. R.A against thickness of films for a set of concentrations (molality).

RESULTS AND DISCUSSION

Permeation

Figure 1 shows a plot of mass flow against the inverse of the thickness of the film. The upper curve represents data from experiments performed under internal to external water activity difference (i.e., the difference between the water activity inside the cup and water activity outside the cup), Δa_w, equal to unity. The lower curves represent data from experiments performed under Δa_w = 0.5. Open symbols represent data from dry cup experiments, closed symbols represent data from wet cup experiments. It can be seen that when Δa_w=1 the same curve is obtained for dry and wet cup experiments, yet when Δa_w = 0.5 the curve for the dry cup experiment is below the curve for the wet cup experiment. The explanation for this result is given next.

Generally, the measured mass flow (J_i^{exp}) of a liquid penetrating through polymer films is the sum of two flows: the Fickian (or diffusive) flow (J_i^d) and the viscous flow (J_i^v). The first, dependent upon the film thickness, corresponds to the activated penetrating transport through the polymer matrix and the second, independent of the film thickness, to transport through frozen holes. We call frozen holes the free volume associated with the discontinuous distribution of microvoids in a gel-like liquid (or glass) after solvent evaporation. In the case of crosslinked polymers like epoxy resins, the holes can also be microregions of low crosslinking density. We assume that these holes are sufficiently large enough to promote capillary penetrating condensation, and so the viscous flow should be controlled only by the penetrating evaporation at the outgoing surface of the film. Normally, it is reasonable to expect the number of microvoids to rapidly decrease with increasing film thickness, but, depending on the solvent evaporation rate, in

many instances these voids could be created as a consequence of solvent retention.

On the other hand, in the case of thin films (generally less than 20 μm thickness), these holes can be described as pinholes, which are constituted by rough defects in films like bubbles, pores, and fissures that could be produced by the deficient application of films, mechanical/thermal stresses, and presence of solid impurities. Also, paint formulations whose pigments are poorly wetted by the resin can lead to debonding at the interface, which will produce pores in paint films. Miscovic et al.[18] referred to these defects as macropores, and showed that they are responsible for electrolyte penetration through films of epoxy resin. By exposure of films to 3% sodium chloride, they found that, although the quantity of electrolyte inside macropores can be only one-tenth of that inside the polymer net, ionic conduction through the film depends only on conduction through macropores. Linoissier et al.,[19] from measurements of water diffusion in polystyrene films, found a non-Fickian behavior, characterized by a fast transport with no time lag. They credited this rapid non-Fickian transport to the presence of defects in the bulk of this material, as they verified by transmission electron microscopy.

At the present, we believe that in thin films, pinholes and frozen holes can coexist, so that the measurement of transport properties in these films can lead to parameters not characteristic of the polymer itself, but of parameters resulting from the transport through rough defects, which are characteristic to the processing. Hence, if one wishes to obtain intrinsic properties of the polymer, measurements should be carried out in thick films, where defects are expected to be almost completely eliminated.

If Fick's first law is obeyed, when the film thickness tends to infinity, the J_i^{exp} value should extrapolate to zero. But if the a polymer matrix that contains a fraction of frozen holes, the J_i^{exp} value, extrapolated to infinite film thickness, is not zero and would correspond to the flow through these frozen holes. Defining this flow as J_i^v:

$$J_i^v = J_i \cdot \frac{A_v}{A_g} \tag{1}$$

where J_i, A_v, and A_g are the penetrating evaporation rate at the experimental temperature, the area corresponding to the fraction of frozen holes, and the geometric area of permeation, respectively. At this point it is important to indicate that once the gel in the liquid is formed, after solvent evaporation, the frozen microvoids are distributed throughout the bulk sample, and so A_v can be considered independent of film thickness.

Let us consider the following equations:

$$J_i^{exp} = J_i^d + J_i^v \tag{2}$$

$$J_i^d = -P_i \cdot \frac{\Delta P_v}{L} \tag{3}$$

where equation (2) and equation (3) define the experimental penetrating flow and Fick's first law, respectively, and P_i, ΔP_v, L are the mean permeability coefficient, the internal to external penetrating vapor pressure difference (i.e., $\Delta P_v = P_{in} - P_{ex}$) and the thickness of the sample, respectively. It is possible to write the diffusive flow (J_i^d), since J_i^v corresponds to the transport through frozen holes and is independent of the film thickness, making $J_i^v = J_i^\infty$.

Therefore:

$$J_i^d = J_i^{exp} - J_i^\infty \quad J_i^v = -\overline{P}i \cdot \frac{\Delta P_v}{L} \tag{4}$$

or rewriting equation (4):

$$\frac{\Delta P_v}{J_i^{exp} - J_i^\infty} = -\frac{L}{P_i} \tag{5}$$

Therefore, if there is a component of viscous flow, then we observe from equation (4) that a plot of J_i^{exp} vs. $1/L$ like that shown in *Figure* 1, when extrapolated until $1/L = 0$, will intercept the ordinate axis at a point that corresponds to J_i^∞. Following this procedure, we obtain in *Figure* 1 the values of J_∞^∞ corresponding to the three curves shown. When $\Delta a_w = 1$, the same value, 0.018 mg/h^{-1}/cm^{-2}, was obtained, for both wet and dry cup experiments. This result shows that when $\Delta a_w = 1$, the water condensed inside the frozen holes, in an extent that is equivalent for both dry and wet cup experiments, such that the same fraction of holes is contributing to viscous flow.

When $\Delta a_w = 0.5$, however, two different values of J_∞^∞ were obtained for wet and dry cup methods. Besides, the values 0.008 mg.h^{-1}.cm^{-2} and 0.004 mg.h^{-1}.cm^{-2} obtained, respectively, for wet cup and dry cup, are small-

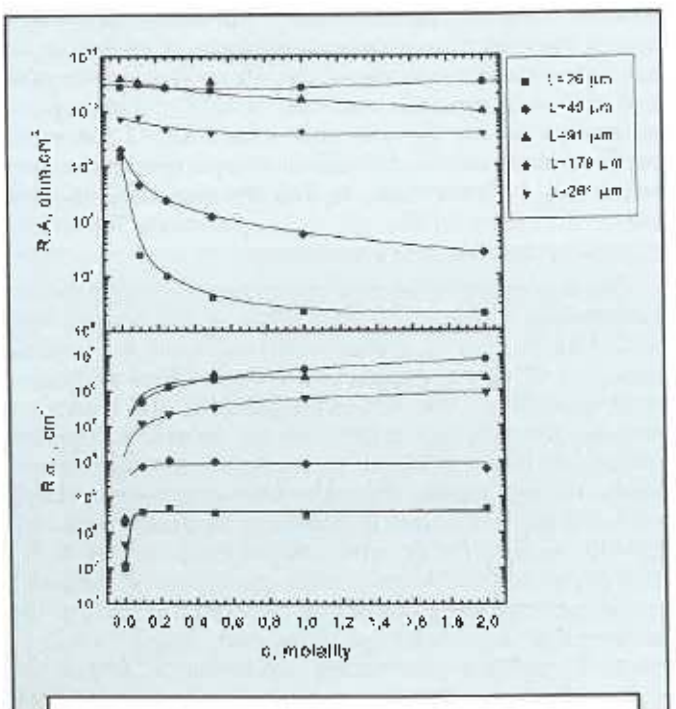

Figure 4—Same data presented in Figure 3, but with concentration as the independent variable. The product of resistance and conductivity of NaCl solution is also included.

er than one-half of that obtained when $\Delta a_w = 1$. This means that, when water activity is less than one, there is less capillary condensation inside the holes, and hence, the viscous flow component is smaller. In addition, when the aqueous solution is in direct contact with the film, as is the case in the wet cup method, a higher value of J_w^v is obtained when compared to that obtained in the dry cup method, because of higher capillary condensation in the former.

Now, using the water evaporation rate value, J (30°C) = 11.63 mg.h^{-1}.cm^{-2} (from measurements in a cup without film), the geometric area of permeation, A_g = 9.07 cm^2, and the value of viscous flow, J_w^v = 0.018 mg.h^{-1}.cm^{-2}, it was possible to determine from equation (1) the area corresponding to the fraction of frozen holes, A_v = 0.014 cm^2. It is important to observe that this area, which corresponds to about 0.15% of geometric area of permeation, although small, is responsible for a significant fraction of mass flow through the films, as can be seen from *Figure* 1. The component of viscous flow J_w^v becomes more significant as the film thickness increases.

From the previous discussion, it becomes clear that one needs to discount from experimental flow the value corresponding to viscous flow, in order to correctly apply Fick's first law to permeation through films. *Figure* 2 shows a master curve obtained after subtracting the viscous flow J_w^v from the measured flow and after correcting for the difference in water activities. Data from *Figure* 1 are represented as $J_w^{exp} - J_w^v$ against $\Delta p_v/L$ in *Figure* 2. With a good approximation, the points fall into a single line. This is what one would expect from a system that obeys Fick's first law, described by equation (3). The slope gives a permeability coefficient of 2.10^{-12} g.s^{-1}.cm^{-1}.mmHg^{-1}. The independence of the permeability coefficient on the water activity, which is revealed by the single slope, shows that the water does not affect the film. Such a result is not unexpected since the films were highly crosslinked after the hard thermal treatment, namely 80°C for 24 hr, as could be estimated by solvent extraction experiments described in the Samples Preparation section.

D.C. Resistance

Data from d.c. resistance measurements are reported in *Figure* 3 as a plot of R.A against thickness of film. R is the measured resistance and A is the area of film exposed to solution, about 5.9 cm^2. Each curve corresponds to a measurement performed at a given NaCl concentration, which is indicated in the graph.

D.C. resistance measurements performed under dry conditions were also included to obtain the intrinsic resistance of the material. It can be seen that intrinsic resistance does not change appreciably within the range of thicknesses studied. Hence, the change in resistance with thickness presented by other curves is caused by the differences in ionic mobility through the films.

In general, the resistances increased with thickness until a maximum of about 100-180 µm and then decreased unexpectedly. The initial increase in resistance

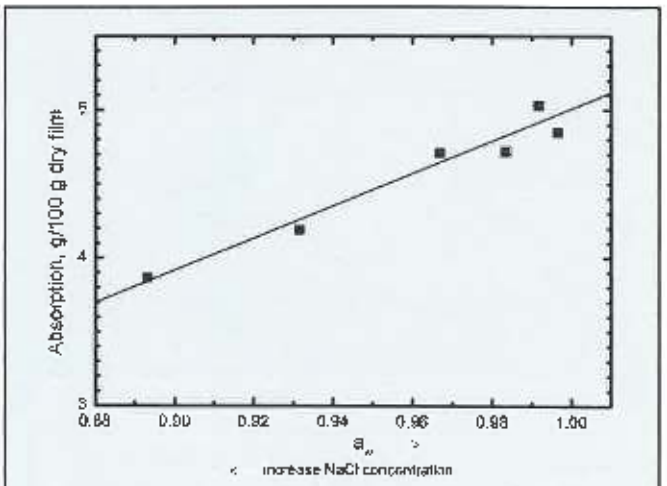

Figure 5 Water absorption against water activity. Films with thickness around 70 µm.

was caused by a reduction in the fraction of pinholes with increasing thickness of the films, as was discussed in the preceding section. The decrease in measured resistance for thicker films could be caused by a reduction in the degree of crosslinking of the films, as a result of solvent retention. In order to verify this supposition, we made solvent extraction measurements. Using acetone as solvent, the mass extracted from films with 23, 45, 74, and 267 µm was respectively 2.5, 2.5, 3.4, and 7.4 g/100 of dry film. As can be seen, thicker films have a higher fraction of soluble material, which means they are less crosslinked. As a consequence of being less crosslinked, thicker films can have a higher fraction of frozen holes,

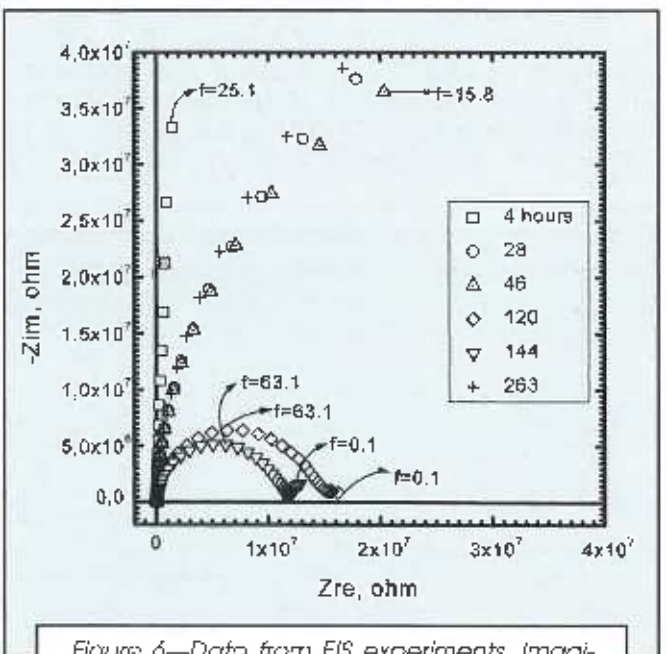

Figure 6—Data from EIS experiments. Imaginary component of impedance (Zim) against real component (Zre). Film with 60 µm. Each curve corresponds to the time exposure indicated by the legend. The variable f displayed at some points indicates the frequency used at that data point.

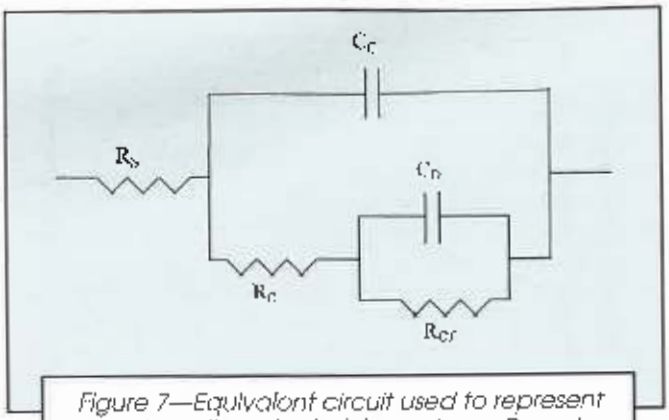

Figure 7—Equivalent circuit used to represent metal-coating-electrolyte system. R_s—solution resistance; C_c—coating capacitance; R_c—coating capacitance; C_D—double layer capacitance; R_{ct}—charge transfer resistance.

which, as we have seen, allow for capillary condensation of water. Ions of sodium and chloride could then be transported through these holes, producing conductive pathways in the films.

In another experiment, we measured sorption of pure water in films with 23, 45, 74, and 267 μm. The uptake of water was respectively 2.2, 3.1, 3.5, and 5.4 g/100 g of dry film. As we can see, thicker films absorb more water as a result of being less crosslinked. On the other hand, thinner, more crosslinked films absorb less water but have a low ionic resistance because of their high fraction of pinholes. Finally, in the range 100-180 μm the epoxy films probably present the optimum balance between high crosslinking and low fraction of pinholes.

Figure 4 presents the same experimental data as shown in *Figure* 3 but with NaCl concentration as the independent variable. The thickness of films is indicated in the legend. The product of the film resistance and conductivity σ of the NaCl solution was also plotted. As can be seen, the resistance, in general, decreases with concentration. This behavior was termed by Mayne et al.[5,6] as conduction type direct (D) because the resistance of the film follows that of external solution. The fall in the resistance with the concentration is high for thinner films because of their high fraction of pinholes, which are filled up with solution, creating conductive pathways through the films. In this case, conductivity depends on electrolyte concentration inside these pathways, which is expected to follow that of external solution.

The total area of these pinholes can be estimated from the plot of R.σ vs. concentration in *Figure* 4, according to the procedure used by Rúvolo-Filho and da Costa.[20] One can consider the polymer film soaked in NaCl solution as a conductivity cell, whose electrodes are separated by a distance L and have an area equivalent to that occupied by pinholes, A_h. This hypothetical cell will have a cell constant given by $R.\sigma = L/A_h$. In *Figure* 3, by extrapolating R.σ values for high concentration regions, where they are nearly constant, one obtains the hypothetical cell constant L/A_h, which can be used to estimate the area of pinholes from the thickness of the film. The calculated values are given in *Table* 1. It can be seen that these areas are much too small when compared to geometric areas of the films, about 5.9 cm^2. Nevertheless, in the case of 26 and 40 μm films, even that small fraction area of pinholes is sufficient enough to produce a pronounced decrease in resistance with concentration, as can be seen in *Figure* 4. This result is in line with that obtained by Miscovic et al.,[18] described in the Permeation Results section.

On the other hand, the area of pathways calculated for the remaining, thicker films is excessively small and is expected to be unrealistic. In fact, pinholes in these thick films are expected to be absent, as we have discussed in permeation experiments, so that ionic transport through them can take place only through frozen holes. Although water can condense inside these frozen holes, ionic concentration and ionic mobility at these sites are probably much lower than that in the external solution. In this case, the values of A_p calculated by the conductivity cell model are underestimated. Indeed, as we have seen, the estimated value for A_p from permeation experiments is 0.014 cm^2 or 1.4×10^6 μm^2, which is much higher than those calculated by the conductivity cell model. Wu et al.,[21] using a wire beam electrode, measured ionic resistance at numerous localized areas (1 mm in diameter) throughout varnish films, finding areas with high resistance (10^{11}-10^{12} ohms) and areas with low resistance (10^6-10^9 ohms). From these measurements, they estimated the percentage of high resistance and low resistance areas of the film. For a phenolic varnish they found 75% of low resistance areas; for an alkyd varnish, 60% of low resistance area; and for a polyurethane varnish, 58% of low resistance area. When comparing these elevated percentages of low resistance areas, with that of only 0.15% for the A_p areas found in the present article, it seems that A_p areas are not related to the low resistance areas found by Wu et al. At this point, it is important to observe that Wu et al. studied very thin films, about 16 μm in thickness, while in the present article films that are considerably thicker were

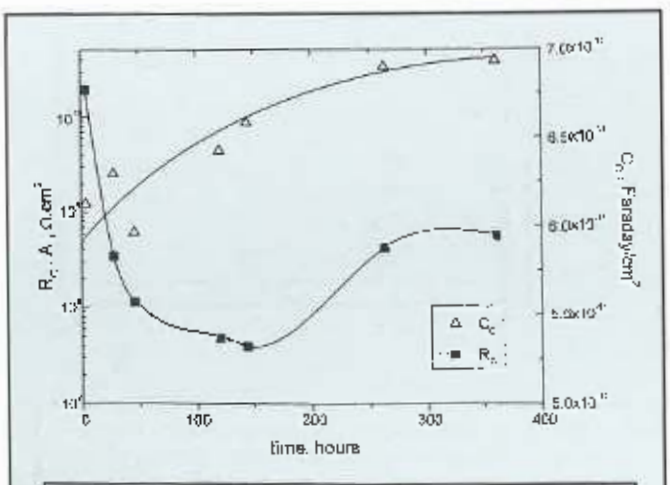

Figure 8—Parameters obtained by fitting the data of Figure 6 to the equivalent circuit given in Figure 7. A—area of film exposed to solution.

studied. Hence, it is reasonable to think that the morphology of the films in the two works are distinct from each other.

From this result, we can presume that ionic transport in thick films of this epoxy resin is highly hindered, although water transport can occur and is easily detectable. This suggests that these films have permeoselectivity, that is, they allow water but not ion uptake, probably due to the presence of fixed charge in the binder matrix. Therefore, the film with 179 μm, which shows the highest resistance, presents a slight tendency to conduction type indirect (I), i.e., its resistance ran counter to that of external solution, as can be seen in *Figure* 4. According to Mayne et al.,[3,6] the increase in resistance with concentration of electrolyte is caused by a reduction in the water content of films due to a decrease in water activity in external solution. *Figure* 5 shows the results of water sorption measurements, where the water uptake is plotted against activity of water in the solution of immersion. The range of activities covered is the same as that used in d.c. resistance measurements. It can be seen that water uptake clearly decreases with a decrease in water activity (increase in NaCl concentration) in the external solution, confirming the aforementioned statement. The sorption experiments were performed in films with thicknesses around 70 μm.

Electrochemical Impedance Spectroscopy

Figure 6 shows the Nyquist representation of the data obtained from a film 60 μm in thickness. This is the typical behavior which is expected from a metal-coating-electrolyte system. In the first hours of exposure to solution, the coating has been slightly penetrated so that it presents, predominantly, a capacitive behavior. Therefore, the plot corresponding to four hours of exposure is almost linear. After 28 hr of exposure, the plot takes a semicircular shape because the uptake of solution into pinholes creates conductive pathways throughout the film, so that the system behaves like an association of capacitors and resistors. *Figure* 7 shows an equivalent circuit often used to represent a metal-coating-electrolyte solution system.[9,12,13] R_c is the coating resistance and C_c is the coating capacitance. Using an appropriate software to fit the data to this model, R_c and C_c could be calculated as a function of exposure time. A plot of (R_c.A) and C_c vs. exposure time is shown in *Figure* 8. As can be seen, initially, in the first 50 hr, the resistance diminishes almost three decades, corresponding to the water imbibition period. However, after about 144 hr of exposure, the resistance increases again because reactions start at the interface metal-polymer. On the other hand, coating capacitance increases as a result of solution uptake until an equilibrium value is reached. Similar behavior was observed for a film with 35 μm.

On the other hand, Nyquist representation of films with 98 and 138 μm remained almost linear when they were exposed to solution, showing only a slight decrease in slope, even after two months of exposure. This is in accordance with d.c. resistance measurements,

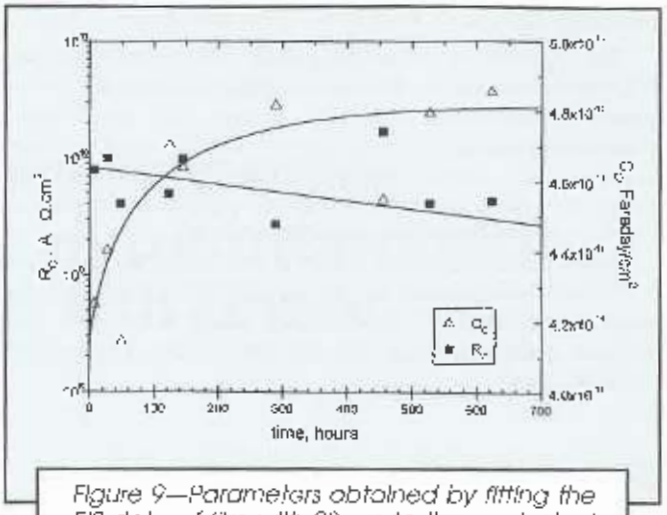

Figure 9—Parameters obtained by fitting the EIS data of film with 98 μm to the equivalent circuit given in Figure 7.

Table 1—Area Covered by Holes (Pinholes and Frozen Holes), A_h, Against Thickness of the Film, L

L, μm	A_h, μm²
26	6.5
40	0.45
91	9.7 x 10⁻³
179	3.6 x 10⁻⁴
261	8.7 x 10⁻⁵

where it was shown that in this range of thicknesses the films present maximum ionic resistance (see *Figure* 3). Hence, in this range of thicknesses permeation of ions through films is highly hindered because pinholes are scarcely present, as one can see from the results in *Table* 1. In *Figure* 9, R_c and C_c for films with 98 μm were obtained as a function of exposure time, using the model shown in *Figure* 7. The uptake of a small amount of solution is noted from the slight decrease in d.c. resistance and slight increase in capacitance. Similar behavior was observed for a film with 138 μm.

The R.A values obtained from d.c. (free films) and a.c. (attached films) measurements are similar when the same thicknesses are compared.

CONCLUSIONS

Results revealed a high dependence of barrier properties of epoxy-polyamide varnish films on their thickness. Thinner films have a significant fraction of pinholes, which are responsible for the failure in the barrier properties of the material. Films relatively thicker, namely 100-150 μm in thickness, when attached to a steel plate are highly impermeable to ions and do not fail in the course of two months of testing. Nonetheless, pathways in the form of frozen holes are still present in thicker films, as we verified from permeation experiments. These frozen holes can be filled with water, but ion mobility and ion concentration at these sites are

probably too small, and so the ionic resistance is high.

The equivalent circuit proposed allows one to obtain R.A values similar to the values obtained from d.c. independent measures. This fact shows that the electrochemical impedance spectroscopy can be used to characterize the ionic transport through the attached polymeric film. The same model of equivalent circuit allows us to explain the aging phenomena.

From a multilayered model it was possible to obtain a Fickian component of the water transport and the mean permeability coefficient, by substracting the non-Fickian component of the transport from the experimental value.

ACKNOWLEDGMENTS

The authors wish to thank CNPq for their financial support of this project and LAC-COPEL for their technical support.

References

(1) Bellucci, F., Nicodemo, L., and Latanision, R.M., *J. Mater. Sci.*, 25, 1097 (1990).
(2) Mayne, J.E.O., *Trans. Inst. Metals Finishing*, 41, 121 (1964).
(3) Kinsella, L.M. and Mayne, J.E.O., *Br. Polym. J.*, 1, 173 (1969).
(4) Mayne, J.E.O. and Scantlebury, J.D., *Br. Polym. J.*, 2, 240 (1970).
(5) Mayne, J.E.O. and Scantlebury, J.D., *Br. Polym. J.*, 3, 237 (1971).
(6) Mayne, J.E.O. and Mills, D.J., *J. Oil & Colour Chemists' Assoc.*, 58, 155 (1975).
(7) Fernández Prini, R. and Corti, H."Epoxy Coal Tar Films: Membrane Properties and Film Deterioration," JOURNAL OF COATINGS TECHNOLOGY, 49, No. 632, 62 (1977).
(8) Corti, H., Baro, G., Fernández-Prini, R., and Maroto, A.G.J., *J. Oil & Colour Chemists' Assoc.*, 61, 75 (1978).
(9) Massiani, Y., Crousier, J.P., and Lazzeri, A., *Corros. Sci.*, 34, 1685 (1993).
(10) Deflorian, F., Pedrizzi, L., and Bonora, P.L., *Corros. Sci.*, 38, 1697 (1996).
(11) Popov, B.N., Alwohaibi, M.A., and White, R.E., *J. Electrochem. Soc.*, 140, 947 (1993).
(12) Van Westing, E.P.M., Ferrari, G.M., and de Wit, J.H.W., *Corros. Sci.*, 36, 957 (1994).
(13) Van Westing, E.P.M., Ferrari, G.M., and de Wit, J.H.W., *Corros. Sci.*, 36, 979 (1994).
(14) McCluney, S.A., Popova, S.N., Popov, B.N., and White, R.E., *J. Electrochem. Soc.*, 139, 1556 (1992).
(15) van der Weijde, D.H., van Westing, E.P.M., and de Wit, J.H.W., *Corros. Sci.*, 36, 643 (1994).
(16) Szauer, T., *Prog. Org. Coat.*, 10, 157 (1982).
(17) Nguyen, T., Hubbard, J.B., and Pommersheim, J.M., "Unified Model for the Degradation of Organic Coatings on Steel in a Neutral Electrolyte," JOURNAL OF COATINGS TECHNOLOGY, 68, No. 853, 43 (1996).
(18) Mitrovic-Stankovic, V.B., Drazic, D.M., and Teodorovic, M.J., *Corros. Sci.*, 37, 241 (1995).
(19) Lmoissier, T., Gailland, F., Romand, M., and Feller, J.F., *J. Appl. Polymer Sci.*, 66, 2465 (1997).
(20) Rúvalo-Filho, A. and da Costa, E.S., "Behavior of Some Anticorrosive Epoxy-Polyamide Primers Free of Lead and Chromate and in the Presence of Chloride Ions," JOURNAL OF COATINGS TECHNOLOGY, 65, No. 818, 67 (1993).
(21) Chi-lan-Wu, Xie-jun Zhou, and Yong-jun Tan, *Prog. Org. Coat.*, 25, 379 (1995).